Design of a graphene–copper hybrid antenna for multiband wireless communication applications

Hassna Agoumi[1*], *Seddik* Bri[2], and *Adil* Saadi[1]

[1]Modeling, Information Processing and Control Systems (MIPCS) National School of Arts and Crafts, Meknes 50000, Morocco
[2]Intelligent Electrical Systems, Materials and Components. High School of Technology, Higher School of Technology, Meknes 50000, Morocco

Abstract. This paper presents a preliminary study of a hybrid graphene–copper microstrip antenna for multiband wireless communication applications. The novelty of the proposed design lies in the integration of conductive graphene strips into a conventional copper patch antenna to improve impedance matching, bandwidth, and radiation characteristics without relying on active switching mechanisms. The antenna performance was investigated using three different substrates, namely Flame Retardant 4 (FR4), Rogers RO4350B, and Rogers RT/duroid 5880 (RT/5880). The graphene layer was modeled using a conductive surface impedance corresponding to its conductive state. Simulated results demonstrate dual-band operation with resonance frequencies located at 1.43 GHz and 2.6 GHz for FR4, 1.5 GHz and 2.8 GHz for RO4350B, and 1.09 GHz and 2.3 GHz for RT5880. The achieved impedance bandwidth ranges from 100 MHz to 200 MHz depending on the substrate properties. Moreover, realized gains of approximately 4 dB for FR4 and 5 dB for both RO4350B and RT5880 were obtained. The results confirm the potential of graphene-assisted antennas for compact sub-6 GHz wireless and Internet of Things (IoT) communication systems.

1 Introduction

The rapid expansion of wireless communication systems and smart connected devices has increased the demand for compact multiband antennas with improved bandwidth and radiation performance. Microstrip patch antennas are widely used in modern wireless applications because of their low profile, low fabrication cost, and ease of integration. However, conventional microstrip antennas generally suffer from limited bandwidth and moderate gain, particularly in compact wireless systems [1, 2].

Recently, graphene has attracted considerable interest in antenna engineering due to its high electrical conductivity, mechanical flexibility, and tunable electromagnetic properties [3, 4]. Several graphene-based antenna structures have been proposed for reconfigurable and high-frequency applications [5]. Nevertheless, most reported studies mainly focus on terahertz or millimetre–wave (mmWave) frequency ranges, while fewer works investigate

[*] Corresponding author: h.agoumi@edu.umi.ac.ma

hybrid graphene–copper microstrip antennas operating in lower wireless communication bands using different dielectric substrates under the same design framework.

In this context, this paper presents the design and simulation of a hybrid graphene–copper microstrip patch antenna using CST Microwave Studio. The proposed structure integrates four graphene strips into a copper patch and is investigated using Flame Retardant 4 (FR4), Rogers RO4350B, and Rogers RT/duroid 5880 substrates. The main contributions of this work include the comparative analysis of the substrate influence on multiband operation, bandwidth, and gain performance, as well as the evaluation of graphene integration effects on antenna radiation characteristics.

2 Modeling Approach

The proposed methodology investigates the effect of graphene integration on the performance of a hybrid graphene–copper microstrip antenna. First, the initial antenna dimensions were calculated using the conventional transmission-line model. Then, four conductive graphene strips were integrated into the copper radiating patch and modeled using the intraband Kubo conductivity model. Finally, the antenna was simulated and optimized in CST Microwave Studio using three dielectric substrates: FR4, Rogers RO4350B, and Rogers RT/duroid 5880.

2.1 Antenna design

The proposed antenna is based on a hybrid graphene–copper microstrip patch structure designed for multiband wireless communication applications. The initial dimensions of the antenna were determined using the conventional transmission-line model, which provides an efficient approach for rectangular microstrip patch design [6].
The patch width is calculated using equation (1):

$$W_p = \frac{c_0}{2f_r\sqrt{\left(\frac{(\varepsilon_r+1)}{2}\right)}} \tag{1}$$

Where W_p is the patch width in (m), f_r is the resonant frequency in (Hz), c_0 is the speed of light in free space in (m s^{-1}), and ε_r is the substrate relative permittivity.

The effective dielectric constant, fringing length extension, effective patch length, and actual patch length are respectively determined using equations (2)-(5) [7]:

$$\varepsilon_{reff} = \frac{\varepsilon_r+1}{2} + \frac{\varepsilon_r-1}{2}\left[1 + 12\frac{h}{W_p}\right]^{-1/2} \tag{2}$$

$$\Delta L = 0.412h\frac{(\varepsilon_{reff}+0.3)\left[\frac{W_p}{h}+0.246\right]}{(\varepsilon_{reff}-0.258)\left[\frac{W_p}{h}+0.8\right]} \tag{3}$$

$$L_{eff} = \frac{c_0}{2f_r\sqrt{\varepsilon_{reff}}} \tag{4}$$

$$L_p = L_{eff} - 2\Delta L \tag{5}$$

Where h is the substrate thickness in (m), ε_{reff} is the effective dielectric constant, ΔL is the fringing length extension in (m), L_{eff} is the effective patch length in (m), and L_p is the actual patch length in (m). The final antenna dimensions were optimized in CST Microwave Studio to obtain the targeted multiband response.

2.2 Graphene conductivity

The electromagnetic behavior of graphene was modeled using the intraband contribution of the Kubo formalism, which is dominant in the gigahertz frequency range [8]. The graphene surface conductivity σs is expressed in equation (6):

$$\sigma_s = \frac{-je^2K_BT}{\pi\hbar^2(\omega-j\tau^{-1})}\left[\frac{\mu_C}{K_BT} + 2ln\left(e^{\frac{-\mu_C}{K_BT}} + 1\right)\right] \tag{6}$$

In this expression the variables involved are as follows: ω: angular frequency (rad.s^{-1}), τ: relaxation time (s), μ_c: chemical potential of graphene (eV), T: absolute temperature (K), e: electron charge (C), $\hbar$: reduced Planck constant (J.s), and k_B: Boltzmann constant (J.K^{-1}). The graphene conductivity mainly depends on the chemical potential, temperature, and relaxation time.

For electromagnetic simulations, graphene was represented by its equivalent surface impedance corresponding to its conductive state, which is related to the graphene conductivity by equation (7) [9]:

$$Zs = \frac{1}{\sigma(\omega,\mu_C,\tau,T)} \tag{7}$$

The applied bias voltage V_b and chemical potential μ_c are related by equation (8) [10]:

$$V_b = \frac{e{\mu_C}^2h}{\pi\hbar^2{v_f}^2\mathcal{E}_0\mathcal{E}_r} \tag{8}$$

In this equation, the variables involved are as follows: V_b: applied bias voltage (V), e: electron charge (C), μ_c: chemical potential of graphene (eV), h: substrate thickness (m), $\hbar$: reduced Planck constant (J.s), v_f : Fermi velocity in graphene (m.s^{-1}), ε_r: relative permittivity of the substrate, and ε_0: permittivity of free space (F.m^{-1}).

To investigate the influence of graphene integration on antenna performance, a hybrid graphene–copper microstrip patch antenna integrating four graphene strips is proposed, as illustrated in Fig. 1.

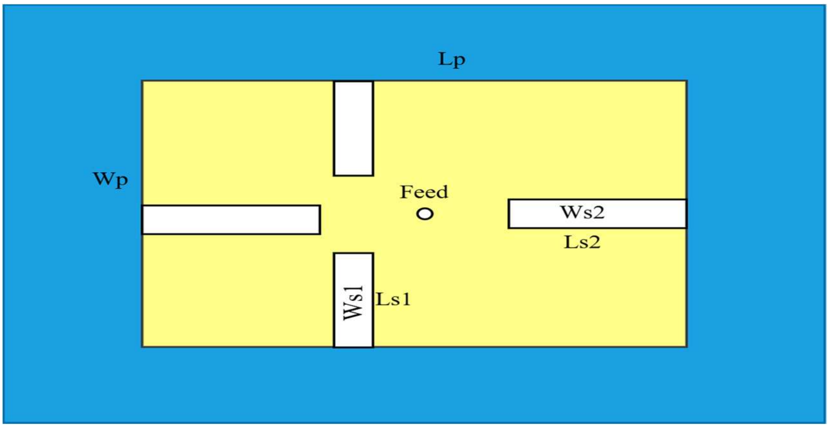

Fig. 1. Geometry of the proposed hybrid graphene–copper microstrip antenna integrating four graphene strips.

The optimized antenna dimensions and the electrical parameters of graphene are summarized in Tables 1 and 2, respectively.

Table 1. Optimized dimensions of the proposed antenna

Parameter	Optimized value (mm)
Patch width (Wp)	37.58
Patch length (Lp)	28.86
Substrate thickness	1.5
Length of strip 1 (Ls1)	2
Width of strip 1 (Ws1)	8.5
Length of strip 2 (Ls2)	11
Width of strip 2 (Ws2)	2

Table 2. Electrical parameters of graphene

Parameter	Value
V_b(V)	21
T (k)	295
τ (ps)	1
Zs (Ω/□)	6.03+j0.1

3 Results and discussion

This section presents the simulated reflection coefficient (S11) and the simulated realized gain of the proposed hybrid graphene–copper antenna for different substrate materials, namely FR4, RO4350B, and RT/5880, using the transient solver of CST Microwave Studio. Graphene was modeled as a conductive surface impedance sheet.

For the FR4 substrate, the antenna exhibits dual-band resonances at 1.43 GHz and 2.6 GHz with bandwidths of approximately 200 MHz and 100 MHz, respectively. The obtained response is suitable for GSM and WiFi wireless communication applications. Using the RO4350B substrate, the resonance frequencies shift to 1.5 GHz and 2.8 GHz with reflection coefficients of approximately −36.9dB and −10.2 dB, respectively. The corresponding bandwidths are around 100 MHz and 200 MHz. The lower dielectric losses of RO4350B improve the impedance matching performance, particularly at the first resonant band. The simulated S11 responses are illustrated in Fig. 2.

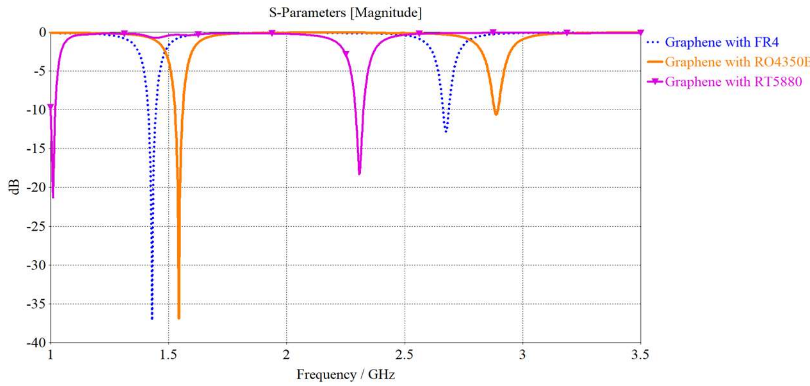

Fig. 2. Simulated S11 responses of the proposed antenna for different substrate materials.

For the RT5880 substrate, the antenna resonates at 1.09 GHz and 2.3 GHz with reflection coefficients of approximately −18.1 dB and −21.27dB, respectively. Bandwidths of about 200 MHz and 100 MHz are achieved for the two operating bands. The RT/5880 has a lower relative permittivity. This shifts the resonances to lower frequencies but does not alter the good impedance matching.

The resonance frequencies, bandwidth, and impedance matching performance of the proposed antenna are significantly affected by the dielectric substrate, as shown by the obtained results; particularly, RT/5880, favors resonance shifting toward lower frequencies and contribute to improved multiband operation.

The simulated realized gain of the proposed antenna for different substrate materials is presented in Fig. 3. The FR4 substrate provides a maximum realized gain of approximately 4 dB around 2.7 GHz. For the RO4350B substrate, the gain reaches nearly 5 dB around 2.9 GHz, while the RT/5880 substrate achieves a maximum gain close to 5 dB near 3.5 GHz.

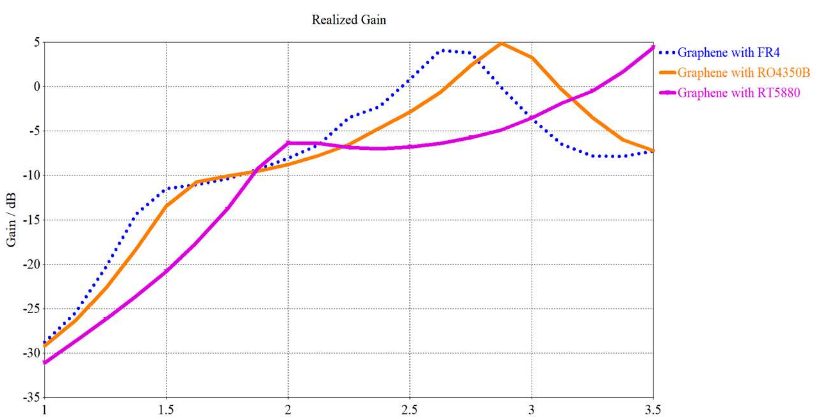

Fig. 3. Simulated realized gain of the proposed antenna for different substrate materials.

The dielectric properties of the substrate strongly influence the antenna gain, according to the obtained results. Due to their lower dielectric losses and better radiation efficiency, the RO4350B and RT/5880 low-loss substrates make it possible to obtain a higher realized gain than FR4. In contrast, the higher loss tangent of FR4 contributes to additional power dissipation, resulting in reduced gain performance. Overall, the proposed antenna demonstrates suitable gain characteristics for multiband wireless communication applications.

4 Comparison with previous studies

Competitive performance compared to recently reported antenna designs is demonstrated by the proposed graphene–copper hybrid antenna, which achieves a peak gain of up to 5 dB when using low-loss substrates. The obtained results in terms of gain, bandwidth, and resonance frequencies confirm the suitability of the proposed structure for multiband wireless communication applications. A comparative analysis with previous studies is summarized in Table 3.

Table 3. Comparison with previous studies

Ref.	Antenna Type	Substrate	Operating Frequency (GHz)	Bandwidth	Peak Gain (dB)	Main Feature
[11]	Dual-band WBAN antenna	Jean textile substrate	2.45 / 5.8	90 MHz / 220 MHz	3.08 / 2.15	Wearable dual-band operation
[12]	Microstrip patch antenna with enhanced coupling	F4B	2.4–3.0	300 MHz	> 4	Wideband response
[13]	Inverse S-shaped meander line antenna	FR4	2.4	210 MHz	1.14	Compact slotted structure
[14]	Moon-shaped reconfigurable patch antenna	FR4	3.29	—	3.08	PIN-diode reconfigurability
This work	Hybrid graphene–copper microstrip antenna	FR4, RO4350B, RT/5880	1.09–2.8	100–200 MHz	Up to 5	Comparative substrate analysis and multiband operation

With a simple geometry, the proposed graphene–copper hybrid structure demonstrates competitive gain and multi-band performance compared to previously reported antennas. Unlike the textile-based WBAN antenna in [11] and the compact FR4 design in [13], which exhibit gains below 3.1 dB, the proposed antenna achieves peak gains up to 5 dB using low-loss substrates. In contrast to the PIN-diode-based reconfigurable antenna reported in [14], the proposed design improves radiation performance without requiring active switching components. Furthermore, the comparative analysis of FR4, RO4350B, and RT/5880 substrates highlights the influence of dielectric properties on bandwidth and impedance matching characteristics.

5 Conclusion

The performance of the proposed hybrid graphene–copper antenna was investigated using FR4, RO4350B, and RT/5880 substrates. The obtained results demonstrated dual-band operation with bandwidths ranging from 100 MHz to 200 MHz and peak gains reaching 5 dB for low-loss substrates. The comparative analysis confirmed that substrate properties strongly influence impedance matching and radiation performance. Furthermore, graphene integration improved the multiband behavior while maintaining a simple antenna structure without requiring active switching components. Although the obtained results are promising, experimental validation and further investigation of tunable graphene parameters remain necessary for future reconfigurable antenna applications.

References

1. M. Shaw, Y. K. Choukiker, Reconfigurable polarization and pattern microstrip antenna for IRNSS band applications. AEU - Int. J. Electron. Commun. **160**, 154501 (2023). https://doi.org/10.1016/j.aeue.2022.154501
2. C. Balamurugan, T. S. Arun Samuel, S. Merlin Gilbert Raj, S. Pricilla Mary, A. Sharon Geege, Enhancing gain and bandwidth in a multiband microstrip patch antenna through L-slot and partial ground plane integration. Sci. Rep. **15**, 29083 (2025). https://doi.org/10.1038/s41598-025-13947-8
3. S. A. M. Alwazzan, A. A. Khamees, M. Al-Rubaye, Designing and simulating of tunable microstrip patch antenna for 5G communications utilising graphene material. J. Commun. **17**, 280–286 (2022). https://doi.org/10.12720/jcm.17.4.280-286
4. M. Mashayekhi, P. Kabiri, A. S. Nooramin, M. Soleimani, A reconfigurable graphene patch antenna inverse design at terahertz frequencies. Sci. Rep. **13**, 8369 (2023). https://doi.org/10.1038/s41598-023-35036-4
5. N. Kiani, F. Tavakkol Hamedani, P. Rezaei, M. Jafari Chashmi, M. Danaie, Polarization controling approach in reconfigurable microstrip graphene-based antenna. Optik **203**, 163942 (2020). https://doi.org/10.1016/j.ijleo.2019.163942
6. Md. S. Rana, Md. M. Rahman Smieee, Design and analysis of microstrip patch antenna for 5G wireless communication systems. Bull. Electr. Eng. Inform. **11**, 3329–3337 (2022). https://doi.org/10.11591/eei.v11i6.3955
7. A. S. A. Gaid, M. A. M. Ali, A. Saif, W. A. A. Mohammed, Design and analysis of a low profile, high gain rectangular microstrip patch antenna for 28 GHz applications. Cogent Eng. **11**, 2322827 (2024). https://doi.org/10.1080/23311916.2024.2322827
8. E. Avşar Aydın, 3D-printed graphene-based bowtie microstrip antenna design and analysis for ultra-wideband applications. Polymers **13**, 3724 (2021). https://doi.org/10.3390/polym13213724
9. B. Zheng, X. Rao, Y. Shan, C. Yu, J. Zhang, N. Li, Multiple-beam steering using graphene-based coding metasurfaces. Micromachines **14**, 1018 (2023). https://doi.org/10.3390/mi14051018
10. A. Hlali, Z. Houaneb, H. Zairi, Dual-band reconfigurable graphene-based patch antenna in terahertz band: design, analysis and modeling using WCIP methode. Prog. Electromagn. Res. C **87**, 213–226 (2018). https://doi.org/10.2528/PIERC18080107
11. W. Thaiwirot, Y. Hengroemyat, T. Kaewthai, P. Akkaraekthalin, S. Chalermwisutkul, A dual-band low SAR microstrip patch antenna with jean substrate for WBAN applications. Int. J. RF Microw. Comput.-Aided Eng. **2024**, 5076232 (2024).

https://doi.org/10.1155/2024/5076232

12. M. T. Khan, X. Q. Lin, C. Zhe, A. Saboor, Design, analysis and validation of a microstrip patch antenna with enhanced coupling for leaf moisture sensing: an IoT approach. Front. Phys. **12**, 1402326 (2024). https://doi.org/10.3389/fphy.2024.1402326
13. S. S. Prottoy, Md. M. Rana, Md. A. Islam, Md. Arifuzzaman, N. Alam, Inverse S-shaped meander line antenna loaded with slotted parasitic patch and defected ground for internet of things (IoT) applications. Prog. Electromagn. Res. C **154**, 31–38 (2025). https://doi.org/10.2528/PIERC24093003
14. S. E. El Aoud, H. Abbaoui, O. Benkhadda, S. Attioui, N. El Assri, S. Ibnyaich, A. Zeroual, M. M. Ismail, A. J. A. Al-Gburi, Design of a crescent moon-shaped reconfigurable patch antenna using a PIN diode for 5G Sub-6 GHz and multistandard wireless applications. Prog. Electromagn. Res. B **109**, 81–93 (2024). https://doi.org/10.2528/PIERB24092501